



# 1 Are cities responsible for their air 2 pollution?

3  
4 Philippe Thunis<sup>1</sup>, Alain Clappier<sup>2</sup>, Alexander de Meij<sup>3</sup>, Enrico Pisoni<sup>1</sup>, Bertrand Bessagnet<sup>1</sup>,  
5 Leonor Tarrason<sup>4</sup>.

6  
7 <sup>1</sup> European Commission, Joint Research Centre, Ispra, Italy

8 <sup>2</sup> Université de Strasbourg, Laboratoire Image Ville Environnement, Strasbourg, France

9 <sup>3</sup> MetClim, Varese, Italy

10 <sup>4</sup> NILU, Norway

11

12 *Correspondence to:* Philippe Thunis (philippe.thunis@ec.europa.eu)

## 13 Abstract

14 While the burden caused by air pollution in urban areas is well documented, the origin of this  
15 pollution and therefore the responsibility of the urban areas in generating this pollution is still a  
16 subject of scientific discussion. Source Apportionment represents a useful technique to quantify  
17 the city responsibility but the approaches and applications are not harmonized, therefore not  
18 comparable, resulting in confusing and sometimes contradicting interpretations. In this work, we  
19 analyze how different source apportionment approaches apply to the urban scale and how their  
20 building elements and parameters are defined and set. We discuss in particular the options  
21 available in terms of indicator, receptor, source and methodology. We show that different  
22 choices for these options lead to very large differences in terms of outcome. In average over the  
23 150 EU large cities selected in our study, the choices made for the indicator, the receptor and the  
24 source each lead to an average factor 2 difference. We also show that temporal and spatial  
25 averaging processes applied to the air quality indicator, especially when diverging source  
26 apportionments are aggregated into a single number lead to favor strategies that target  
27 background sources while occulting actions that would be efficient at the city center. We stress  
28 that methodological choices and assumptions most often lead to a systematic and important  
29 underestimation of the city responsibility, with important implications. Indeed, if cities are seen  
30 as a minor actor, plans will target in priority the background at the expense of potentially  
31 effective local actions.

32

33 **Keywords:** air pollution, source apportionment, particulate matter

34

## 35 1. Introduction

36 About 55% of the world's population lives in urban areas nowadays, and this number is expected  
37 to increase to 68% by 2050, according to the United Nations (UN 2018). Large population  
38 growth is also projected by 2030 in most of the major European cities (Alberti et al., 2019) with  
39 predicted population growth varying in range from Berlin (15%), Paris (19%), Milan/Rome  
40 (21%), Prague (37%), London (39%), to Brussels (52%) (see  
41 <https://urban.jrc.ec.europa.eu/thefutureofcities/urbanisation#the-chapter>). As a result of this



42 population trend, urban emissions and their associated pollution levels are expected to increase  
43 as well.

44

45 According to a recent estimate (EEA, 2020), about 74 % of the EU-28 urban population are  
46 exposed to pollution of fine particulate matter (PM<sub>2.5</sub>) in concentrations above the WHO Air  
47 Quality Guidelines value, this number raises to 99% for ozone (O<sub>3</sub>) and is about 4% for nitrogen  
48 dioxide (NO<sub>2</sub>). Air pollution is a heavy burden on human health with more than 380,000  
49 premature deaths in EU-28 reported in 2017 according to the same EEA estimates. For a wide  
50 range of European cities, Khomenko et al. (2021) showed that the health burden due to air  
51 pollution varies greatly by city, with annual premature mortality reaching up to 15% for PM<sub>2.5</sub>  
52 and 7% for NO<sub>2</sub>. The highest mortality burden for PM<sub>2.5</sub> occurs in northern Italy, southern  
53 Poland and eastern Czech Republic. De Bruyn and de Vries (2020) showed that for all 432 cities  
54 in their sample (total population: 130 million inhabitants), the social costs (e.g. hospital  
55 admissions, premature mortality) but also due to air pollution exceeded € 166 billion in 2018 for  
56 Europe (EU27 plus the UK, Norway and Switzerland). City size was shown to be a key factor  
57 contributing to the total social costs: all cities with a population over 1 million features in the  
58 Top 25 cities with the highest social costs due to air pollution.

59

60 Given the health and economic burden caused by air pollution in urban areas, it is important to  
61 identify the origin of this pollution in order to reduce and control its impact. Identifying the  
62 sources of urban pollution and then assigning responsibilities enables a process to implement  
63 measures and control air pollution. Assessing the responsibility or share of cities for their  
64 pollution has important implications. For being effective, pollution reduction plans must be  
65 designed and applied to target the most polluting sectors at the relevant spatial (national, regional  
66 and/or local) and with the appropriate temporal scales. In this context, quantifying the share or  
67 the city pollutions caused by their own emissions becomes a crucial element to determine  
68 whether actions need to be applied locally or at the regional, national country or continental  
69 scales. This has important governance consequences for the effective control of air pollution.

70

71 For pollutants like NO<sub>2</sub>, that mostly originate from traffic sources and have a relatively short  
72 lifetime in the atmosphere, there is a general agreement on the fact that cities are the main  
73 contributor to this pollutant concentration levels and that acting locally on traffic emissions is the  
74 most efficient way of improving NO<sub>2</sub> concentration levels in a particular city (Tobias et al.,  
75 2020). There is available European-wide information such as in Degraeuwe et al. (2019)  
76 providing overviews of the potential impact of traffic emission reductions per vehicle type in  
77 different European cities. There is also agreement regarding O<sub>3</sub> that this secondary pollutant is  
78 most effectively reduced by implementing reduction measures at larger spatial scales, involving  
79 actions driven at the regional and even continental scales (e.g. Luo et al. 2020). For other  
80 pollutants, like PM<sub>2.5</sub>, complex physical and chemical atmospheric processes with different time  
81 scales drive its formation, involving numerous precursors themselves emitted by several sources.  
82 The sources of PM<sub>2.5</sub> pollution range from local traffic, domestic fuel burning and industrial  
83 activities to regional sources such as agriculture in rural areas. Even though the latter emissions  
84 do not originate from cities, Thunis et al. (2018) showed that their impact on urban pollution  
85 could be important, reaching up to 30% in several European cities. Because of this complexity,  
86 there is less consensus regarding the responsibility or share of a city to its pollution when



87 addressing PM<sub>2.5</sub>. Because of this lack of consensus and the major burden of PM<sub>2.5</sub> on health, we  
88 focus our analysis on this pollutant.

89  
90 The usual approach to assess the city share to its pollution levels (in other words the city  
91 responsibility) is source apportionment (SA). However, many SA approaches exist and many  
92 ways to parameterize them as well, leading to a variety of results and interpretations. The most  
93 widely used SA methods are the “potential impact” (or brute force), the “increment” and  
94 “tagging” approaches. An overview description of these methods and an evaluation of their  
95 limitations and capabilities for use can be found in Thunis et al. (2019). For the 18 million  
96 inhabitant’s city of New Delhi, Amann et al. (2017) concluded that only 40% of the PM<sub>2.5</sub>  
97 pollution was originating from local city sources, based on potential impacts SA and expressed  
98 in terms of city averaged population exposure, averaged yearly. In the context of the Copernicus  
99 programme, CAMS (Copernicus Atmosphere Monitoring Service) performs SA calculations  
100 daily with two different approaches, namely tagging and potential impacts, for a series of  
101 European cities. Results show important differences on a day-by-day basis although these  
102 differences smooth out when considering longer term averages (Pommier et al. 2020). Based on  
103 the increment approach, Kiesewetter and Amann (2014) derived SA estimates for a series of  
104 European cities and aggregated these detailed results at country levels, leading to relatively low  
105 city responsibilities (e.g. about 25% for French, German or Italian cities). Based on a potential  
106 impact approach, Thunis et al. (2018) estimated city shares for 150 cities in Europe. They  
107 highlighted their large variability across Europe and stressed the importance of the definition of  
108 the city on the results, by testing the sensitivity to different city extensions. The choice of the SA  
109 method but also the way this method is configured, can lead to very different outcomes for the  
110 city share to its pollution, ranging from cities being a major contributor to their pollution to cities  
111 having a limited responsibility. This explains why the actual city responsibility on its pollution is  
112 yet discussed, and why some authors stress the importance of local actions (Thunis et al., 2018,  
113 Wu et al. 2011, Raifman et al., 2020) when others stress the need for regional, national or even  
114 continental actions (ApSimon et al. 2021, Liu et al., 2013). This diversity of conclusions has  
115 serious consequences in terms of policy decisions. Blaming external (i.e. outside the city)  
116 pollution sources as main responsible for urban pollution is sometimes an easy argumentation for  
117 decision-makers to justify local inaction.

118  
119 This work aims at explaining the main causes of discrepancies between different assessments of  
120 the city emission’s impact on its pollution levels and show that these discrepancies generally lead  
121 to underestimating the city’s responsibility. It proposes a specific harmonized nomenclature for  
122 source allocation approaches, and it shows how it is important to document the choices to enable  
123 correct interpretation of the results. We begin with a conceptual overview of the parameters  
124 structuring any SA approach (Section 2). This includes the definition of the key parameters to  
125 any SA study: indicator, source, receptor, and methodology to relate them. Then (Section 3) we  
126 assess the sensitivity of the urban SA results to the choices of these four parameters. In Section  
127 4, we analyze implications in terms of air quality planning and suggested strategies. We finally  
128 provide conclusions in Section 5.

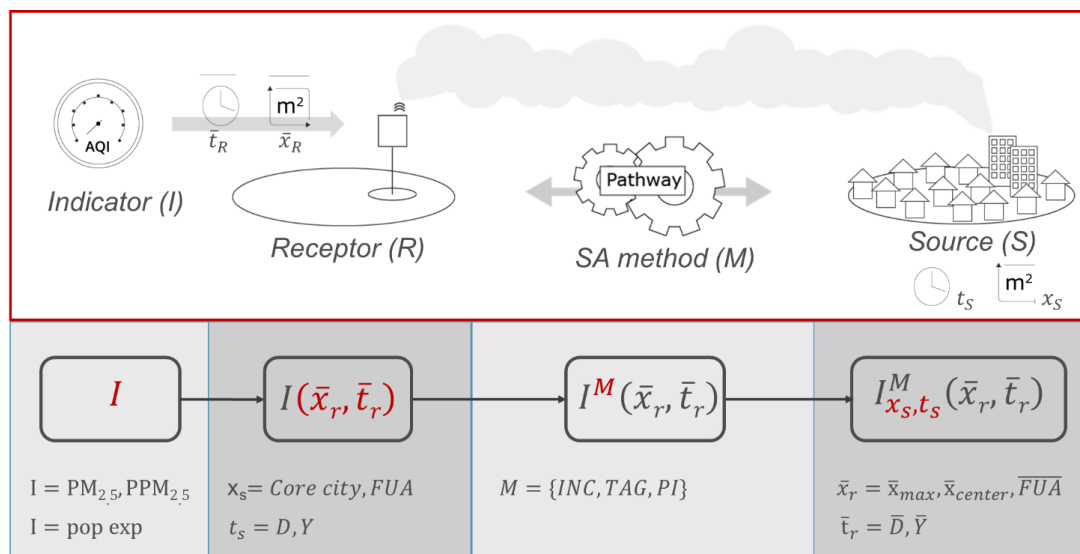
## 129 2. Assessing the city responsibility on air pollution: Main concepts

130 In this section, we detail the steps required to quantify the responsibility of a city on its air  
131 pollution, through source apportionment (SA). SA is a methodology that serves to estimate the



- 132 contribution of a given source at a specific receptor for a given indicator (for example the  
 133 concentration of a given pollutant like PM or NO<sub>2</sub>). It involves the following steps (Figure 1):  
 134  
 135 (1) defining a relevant indicator, denoted as (I) to characterize air pollution  
 136 (2) defining the receptor (R) through its spatio-temporal characteristics, i.e. the area ( $\bar{x}_R$ )  
 137 and time period ( $\bar{t}_R$ ) over which the indicator is averaged  
 138 (3) defining the source (S) through its spatio-temporal characteristics, i.e. the city area  
 139 ( $x_S$ ) and time period for which the city responsibility is assessed ( $t_S$ )  
 140 (4) selecting the source apportionment (SA) methodology to capture the processes that  
 141 relate the source to the receptor.

142 Figure 1 summarizes these steps, as well as the nomenclature and symbols used in this work. We  
 143 use this new nomenclature to attach contextual information (i.e. metadata) to the source  
 144 apportionment. Further explanations of the symbols are given in the subsections below.  
 145



146  
 147 Figure 1: Schematic flow chart representing the four steps required to fully define any SA process. The red letters indicate the  
 148 indicator characteristic under consideration. The general notation for the indicator (I) includes a superscript for the  
 149 methodological approach (M), a subscript to inform on the source (S) and brackets to inform on the receptor (R). The spatial and  
 150 temporal dimensions associated to the source and receptor are denoted by "x" and "t", respectively. The overbar indicates an  
 151 averaging process. The lowest row provides for each parameter examples used in this work.

## 152 2.1 Definition of the air pollution indicator (I)

153 The first step required to assess the role/responsibility of city emissions with respect to its air  
 154 pollution, is to define an indicator that identifies the pollution aspect we are interested in. The  
 155 indicator can be defined in many ways. For example, as the total concentration of a given  
 156 compound (e.g. PM), or as a specific constituent of that total concentration (e.g. PM<sub>2.5</sub> or its  
 157 primary fraction, PPM), or as a composite based on a mix of different pollutants (e.g. maximum  
 158 among O<sub>3</sub>, PM<sub>2.5</sub> and NO<sub>2</sub> concentrations as in some air quality indexes such as ATMO2003) or  
 159 as population exposure (i.e. product of population and concentration).



## 160 2.2 Definition of the receptor (R)

161 Estimating the indicator, either from a measuring instrument or from a model simulation, implies  
162 an averaging process, both in space and time. For model data, averages correspond to the spatial  
163 and temporal resolutions (e.g. the time step and grid cell size) whereas for measurement, the  
164 space-time average will depend on the instrument acquisition time and on the atmospheric  
165 dispersion characteristics at the measuring site. Regardless of these intrinsic time and space  
166 averages, indicators are generally averaged over longer spatial and temporal scales for  
167 convenience. The receptor is defined as the spatio-temporal entity over which the indicator is  
168 averaged. Both a spatial and a temporal scale (denoted by  $\bar{x}_r$  and  $\bar{t}_r$ , respectively) must be  
169 associated to the receptor to define it.

170  
171 For the temporal dimension, typical examples for PM<sub>2.5</sub> are days ( $\bar{t}_r = \bar{D}$ ) or years ( $\bar{t}_r = \bar{Y}$ ).  
172 Spatially, the indicator can be estimated at a specific location, e.g. the city center ( $\bar{x}_r = \bar{x}_{center}$ ),  
173 at the location where the maximum concentration occurs ( $\bar{x}_r = \bar{x}_{max}$ ) or averaged over the city  
174 ( $\bar{x}_r = \overline{city}$ ). For convenience, we use indifferently the following notations to refer to the  
175 receptor:

$$176 R(\bar{x}_r, \bar{t}_r) = R = \bar{x}_r, \bar{t}_r \quad (1)$$

## 177 2.3 Definition of the source (S)

178 The source is defined as the spatio-temporal entity for which we assess the contribution to the  
179 indicator. For the purpose of this work, the source is defined as the city, and more precisely as  
180 the emissions that originate from a given city. The source emissions (denoted by E) are indeed  
181 responsible for the pollution fraction that can be associated to the source/city at the receptor (R).  
182 These emissions are characterized by a spatial ( $x_s$  = extension of the city) and a temporal scale ( $t_s$   
183 = period of time over which the source activity is assessed). For convenience, we use  
184 indifferently the following notations to refer to the source:

$$185 S(x_s, t_s) = S = E = city = x_s, t_s \quad (2)$$

186  
187 In this work, we analyse in particular the impact of the city extension ( $x_s$ ) on the apportionment  
188 outcome. For this purpose, we define cities in two ways:

- 189  
190 (1) as core cities, i.e. the local administrative units, with a population density above  
191 1500/km<sup>2</sup> and a population above 50,000, where the majority of the population lives in an  
192 urban center and  
193 (2) as functional urban areas (OECD, 2012, denoted as “FUA”) composed as core cities plus  
194 their wider commuting zone, consisting of the surrounding travel-to-work areas where at  
195 least 15% of the employed residents work in the city.

196 Details on the FUA and core city areas are available for 150 EU cities in the urban PM<sub>2.5</sub> atlas  
197 (Thunis et al. 2017). Note that other city definitions exist. In the context of the CAMS source  
198 allocation analysis, city are defined as an arbitrary number of grid cells in the modelling domain  
199 (Pommier et al., 2020).



200 Finally, we define the city background as the sum of all contributions from sources that are not  
201 covered by the spatial ( $x_s$ ) and temporal ( $t_s$ ) scales of the city source.

202  
203 One main difference between sources and receptors is that for the latter, spatio-temporal  
204 characteristics are averaged. Apart from this, temporal and spatial characteristics can also differ  
205 in terms of value. For example, the source can be defined as the FUA ( $x_s = \text{FUA}$ ) while the  
206 receptor is a specific location ( $\bar{x}_r = \bar{x}_{max}$ ). Temporally, interest can be on assessing the  
207 contribution of the city weekly activity ( $t_s = 1$  week) for a given day ( $\bar{t}_r = \bar{D}$ ) at the receptor. In  
208 the results presented here, the source and receptor temporal scales are however chosen identical  
209 for convenience.

## 210 2.4 Selection of the SA methodology

211 When the air pollution indicator and the spatio-temporal characteristics of both the receptor and  
212 the source have been selected, the next step consists in distinguishing and quantifying the  
213 fractions of the indicator related to the city source ( $I_{city}(R)$ ) and to the background ( $I_{bg}(R)$ ) at  
214 receptor R, respectively. This decomposition is summarized by the following equation:

215

$$I(R) \rightarrow \{I_{city}(R), I_{bg}(R)\} \quad (3)$$

216

217 Different SA methodologies exist to perform this operation. In this section, we describe three  
218 main approaches but only in brief, as details about each of these are discussed in other works  
219 (Clappier et al. 2017; Thunis et al., 2019, 2018; Mertens et al. 2018). As mentioned previously,  
220 we use the indicator's superscript to refer to its calculation method [ $I_{city}^M(R)$ ]. Methods are  
221 summarized in Table 1.

222

223 **Potential impacts (PI):** The city contribution in this method is denoted as  $I_{city}^{PI100}(R)$  and is  
224 calculated as the difference between two simulations: a base-case that includes the city  
225 [ $I(R)$ ] and a scenario in which the city emissions are switched off [ $I_{city}^{100}(R)$ ]. In this notation,  
226 the source superscript (here, 100) indicates the percentage intensity by which the source  
227 emissions are reduced. Reductions are intended as percentage variations from the base-case  
228 situation. The same approach can be used with reduction percentages that are lower than 100%.  
229 In this case the resulting difference is divided by the reduction percentage to obtain the potential  
230 impact ( $I_{city}^{PI\alpha}(R)$ ). A similar approach is used to calculate the background contribution, i.e. by  
231 removing or reducing partially the background emission sources. Potential impacts methods for  
232 source apportionment are widely used (Osada et al. 2009; Huang et al. 2018; Wang et al. 2014;  
233 Wang et al. 2015; Van Dingenen et al. 2018; Thunis et al. 2016; Clappier et al. 2015; Pisoni et al.  
234 2017).

235

236 **Increment (INC):** With this methodology, the background contribution is estimated as the  
237 concentration observed/modelled at a given location “y” [ $I_{bg}^{INC}(R) = I(\bar{y}, \bar{t}_r)$ ]. This location must  
238 be far enough from the source, not to feel its influence but be close enough to the source to avoid  
239 influences from other sources, external to the city. These assumptions are further described and  
240 discussed in Thunis et al. (2017). The city contribution is then obtained as the difference between  
241 the base case indicator and the background contribution [ $I_{city}^{INC}(R) = I(\bar{x}_r, \bar{t}_r) - I(\bar{y}, \bar{t}_r)$ ]. The  
242 increment methodology has been used e.g. by Lenschow et al. (2001), Petetin et al. (2014),



243 Kieseewetter et al. (2015), Squizzato et al. 2015, Timmermans et al. 2013, Keuken et al. 2013,  
 244 Ortiz and Friedrich 2013 and Pey et al. 2010.  
 245  
 246 **Tagging (TAG):** With this approach, species emitted by the city are numerically tagged and  
 247 followed through the modelled transport, dispersion and chemical transformation processes.  
 248 When chemical transformations take place, preserved atoms are used as tracers. For example, the  
 249 nitrogen atom (N) will be used to follow the NO source emissions through its successive  
 250 transformations into NO<sub>2</sub> and HNO<sub>3</sub> to reach its final product NO<sub>3</sub>, that will then be attributed to  
 251 that source. Example of tagging applications are e.g. Kranenburg et al. 2013, Yarwood et al.  
 252 2004; Wagstrom et al., 2008; Kwok et al. 2013; Bhave et al. 2007; Wang et al., 2009. Some of  
 253 these approaches are implemented operationally to estimate daily city contributions on air  
 254 pollution (<https://topas.tno.nl/documentation/>).  
 255  
 256 The formulations corresponding to these three main approaches are summarized in Table 1.  
 257  
 258 A few key points are worth noting. While tagging and potential impacts approaches explicitly  
 259 consider city emissions in their calculations, this is not the case for increments that only refer to  
 260 them implicitly. By construction, both the increment and tagging approaches are additive [i.e.  
 261  $I(R) = I_{city}(R) + I_{bg}(R)$ ] whereas this is not the case for potential impacts when pollutants  
 262 behave non-linearly because of air transport, deposition or chemical processes (Clappier et al.,  
 263 2017).  
 264  
 265

	City contribution	Background contribution
<b>Potential Impact</b>	$I_{city}^{PI\alpha} = \frac{I(R) - I_{city}^{\alpha}(R)}{\alpha}$	$I_{bg}^{PI\alpha} = \frac{I(R) - I_{bg}^{\alpha}(R)}{\alpha}$
<b>Increment</b>	$I_{city}^{INC} = I(\bar{x}_r, \bar{t}_r) - I(\bar{y}, \bar{t}_r)$	$I_{bg}^{INC} = I(\bar{y}, \bar{t}_r)$
<b>Tagging</b>	$I_{city}^{TAG} = \sum_E^{city} I_E(R)$	$I_{bg}^{TAG} = \sum_E^{bg} I_E(R)$

266 *Table 1: Formulation of the three main methods to estimate the contribution/impact/increment of a city. The letters, I, S and R*  
 267 *refer to the indicator, source and receptor, respectively. The indicator superscript refers to the SA method (PI for potential*  
 268 *impacts, INC for increments and TAG for tagging) while its subscript indicates the source (city or background (bg)).  $\alpha$  represents*  
 269 *the percentage reduction factor applied for the source emissions in the potential impacts method. See text for additional details.*

### 270 3. Results

271 Recognizing the impossibility of assessing the sensitivity of the results for all combinations of  
 272 indicators, source, receptor and methodology, we focus our analysis on comparisons in which



273 only one parameter is changed at a time, to highlight major sensitivities. For this purpose, we use  
274 the following two main sources of data and results.

275

276 • SHERPA: SHERPA is a modelling tool, based on Source-Receptor Relationships that  
277 represent a simplified version of a Chemistry Transport Model, used to simulate the  
278 contribution to PM<sub>2.5</sub> concentration levels by all precursor emissions (NO<sub>x</sub>, NMVOC,  
279 PPM, SO<sub>2</sub> and NH<sub>3</sub>) from different cities in Europe (Clappier et al. 2015, Thunis et al.  
280 2016, 2018). In its current configuration, SHERPA is based on the CHIMERE model  
281 (Menuet et al. 2013) covering the whole of Europe at roughly 7 km spatial resolution. In  
282 this work, we use the source apportionment results over 150 cities as reported in the  
283 PM<sub>2.5</sub> urban atlas (Thunis et al., 2017) as well as additional SHERPA data to provide  
284 further analysis.

285

286 • EMEP simulations: The EMEP model is an off-line regional transport chemistry model  
287 (Simpson et al., 2012; <https://github.com/metno/emep-ctm>). The model has 20 vertical  
288 levels, with the first level around 50 m. The model uses meteorological initial conditions  
289 and lateral boundary conditions from the European Centre for Medium Range Weather  
290 Forecasting (ECMWF-IFS). The meteorological year is 2015. Detailed information on  
291 the meteorological driver, land cover, model physics and chemistry are described in  
292 Simpson et al. (2012) and in the EMEP Status Report 2017  
293 ([https://emep.int/publ/reports/2017/EMEP\\_Status\\_Report\\_1\\_2017.pdf](https://emep.int/publ/reports/2017/EMEP_Status_Report_1_2017.pdf)). In this work, we  
294 use specific simulations where emissions have been removed partially or fully in a series  
295 of European cities. Additional details regarding these simulations are provided together  
296 with the discussion of the results.

297 Based on these sources of information and data, we discuss hereafter the sensitivity of the SA  
298 results to the choice of the indicator (Section 3.1), to the choice of the methodology (Section  
299 3.2), to the source (Section 3.3) and finally to the receptor (Section 3.4).

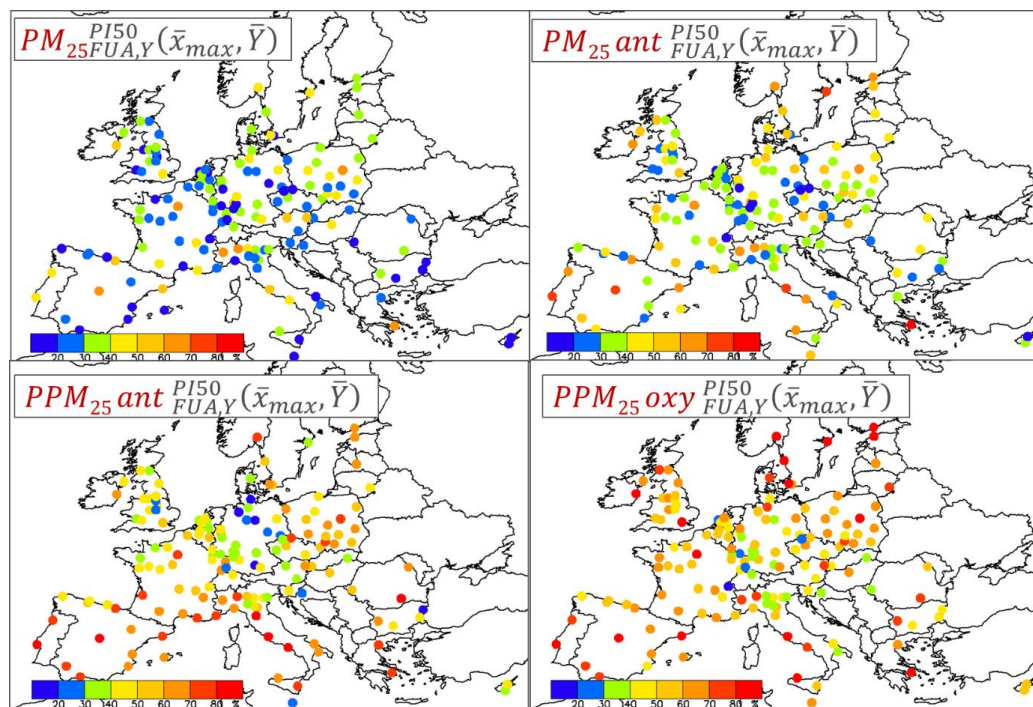
### 300 3.1 Sensitivity to the indicator

301 The implications resulting from the choice of the indicator are illustrated in Figure 2 for four  
302 indicators, based on SHERPA results for 150 cities in Europe. The four indicators selected to  
303 characterize air pollution are: a) the PM<sub>2.5</sub> concentration (top left, from Thunis et al. 2017), b) the  
304 anthropogenic fraction of PM<sub>2.5</sub> (“PM<sub>2.5</sub> ant”, top right), c) the primary anthropogenic fraction of  
305 PM<sub>2.5</sub> (“PPM<sub>2.5</sub> ant” bottom left) and d) the primary fraction of PM<sub>2.5</sub> originating from the  
306 transport and residential sectors (“PPM<sub>2.5</sub> oxy”, bottom left). The reference (PM<sub>2.5</sub> total mass, top  
307 left) corresponds to the indicator currently used in legislation (e.g. European Ambient Air  
308 Quality Directive, AAQD2008) against which health impacts are correlated (WHO2005). In the  
309 second case, the indicator is limited to its anthropogenic fraction (PM<sub>2.5</sub> ant), excluding therefore  
310 natural contributions (dust, marine salt...). This is motivated by the fact that policies have no  
311 impact on this component. According to this indicator, city contributions increase significantly  
312 (by about 20% in average) and in some cities where natural dust pollution is important (e.g. in  
313 Sicily), the city responsibility shifts from minor to major. If we further restrict the indicator to its  
314 primary anthropogenic fraction (“PPM<sub>2.5</sub> ant”, bottom right) because of its suggested higher  
315 health burden (Park et al., 2018; Viana et al., 2008), the city contribution then increases





316 significantly in most cities. This becomes even more striking if we limit the indicator to the  
317  $PM_{2.5}$  fraction originating from the transport and residential sectors (bottom right). These two  
318 sectors have recently been shown to generate the largest burden on human health given the high-  
319 oxidative potential of their emissions (Rankjar et al., 2020, Li et al. 2016). With this indicator,  
320 the majority of EU cities become main contributors to their pollution. Regarding the latter  
321 indicator, it is important to note that although the increasing adoption of electric vehicles shows  
322 rather positive impacts on health (Choma, 2020), the remaining PM emissions from road traffic  
323 like tires and brake and road wear emissions (Kole et al., 2017; EC, 2014; Ntziachristos and  
324 Boulter, 2019) will remain an issue. The calculation of various geochemical indices (enrichment  
325 factor, geo-accumulation index, pollution index and potential ecological risk) also show that road  
326 dust is extremely enriched and contaminated by elements from tire and brake wear (e.g. Sb, Sn,  
327 Cu, Bi and Zn).  
328



329  
330 Figure 2: SHERPA results for 150 major cities in Europe for the overall  $PM_{2.5}$  concentration (top left), for its anthropogenic  
331 fraction (“ $PM_{25\_ant}$ ”, top right), for its anthropogenic primary fraction (“ $PPM_{25\_ant}$ ”, bottom right) and for its primary  
332 fraction originating from the transport and residential sectors (“ $PPM_{25\_oxy}$ ”, bottom left). For all cities, the source is defined  
333 spatially as the FUA over which emissions are reduced every a year (Y). The receptor is defined as the city location where the  
334 concentration is maximum ( $\bar{x}_{max}$ ) and the indicator is averaged yearly at the receptor ( $\bar{Y}$ ). All calculations are made with the  
335 same SA methodology, namely, potential impacts (PI) with city emissions reduced by 50% (PI50)

### 336 3.2 Sensitivity to the SA methodology

337 A comparison of SA methodologies is proposed in Thunis et al. (2019) where the potential  
338 impact, increment and tagging approaches are compared both on simple theoretical examples and  
339 on real data to highlight differences among methods and stress their limitations. In this section,  
340 we summarize the main findings of this work and complement it with comparisons that focus on



341 the apportionment of the city vs. background contributions. We also provide in the appendix a  
342 comparison of all SA methods discussed in this section, applied on a theoretical example tuned  
343 to the city scale.

344

#### 345 Increment vs. potential impacts

346

347 Thunis (2017) compared increments and potential impacts with the SHERPA model for a series  
348 of European cities. They showed that increment approaches lead to important underestimations  
349 (30 to 50%) of the city responsibility for PM<sub>2.5</sub> and NO<sub>2</sub> with respect to potential impacts. This  
350 underestimation is explained by the non-fulfilment of the two underlying increment assumptions,  
351 related to the external location [i.e.  $y$  in  $I_{bg}^{INC}(R) = I(\bar{y}, \bar{t}_r)$ ] that must: 1) be far enough from the  
352 city, not to feel its influence but 2) close enough to the city to avoid influences from sources  
353 external to the city. The Authors show that these two assumptions are seldom fulfilled in reality.

354

#### 355 Tagging vs. potential impacts

356

357 Clappier et al. (2017) discussed the concepts underlying these two SA methods and showed that  
358 important differences in terms of results arise as soon as non-linear processes are present. Belis  
359 et al. (2020) highlighted and quantified these large differences based on a real-case inter-  
360 comparison exercise. Finally, Thunis et al. (2019) reviewed in their work many inter-  
361 comparisons between tagging and potential impact SA results. In their application over the Po  
362 basin (Italy), they showed that differences are large for the agriculture sector (dominated by NH<sub>3</sub>  
363 emissions) but are also important for other sectors, when dealing with high temporal resolution  
364 (e.g. daily) at the receptor. Unfortunately, these examples did not address the particular case of a  
365 city scale apportionment.

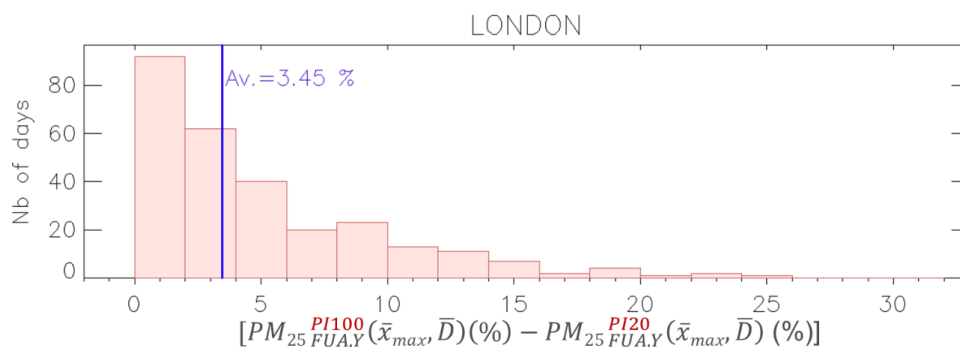
366

#### 367 Full vs. partial potential impacts

368

369 To analyze differences between full and partial impacts, we use a series of EMEP simulations in  
370 which we remove totally (PI100) or partly (PI20) the London FUA emissions (source) during an  
371 entire year. Figure 3 shows the differences between city contributions obtained with the two PI  
372 methods. Differences can be important (up to 25 percentage points for specific days). Although  
373 the number of high-difference days is limited (leading to a yearly average difference of few  
374 percents), these days might represent high pollution episodes for which assessing the city  
375 responsibility is important to act. In general, the higher resolution applied to the temporal and/or  
376 spatial averages at the receptor, the largest the differences are among methods. It is also  
377 interesting to note that partial potential impacts systematically underestimate full potentials (no  
378 negative values).

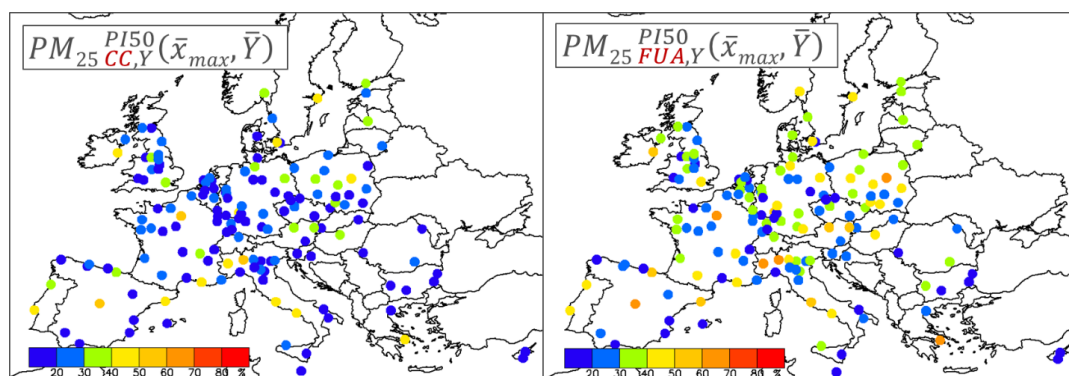
379



380  
381  
382  
383  
384  
385  
Figure 3: Histogram of daily city contribution differences to London  $PM_{2.5}$  levels between two potential impacts methods,  $PI_{100}$  and  $PI_{20}$ , calculated with the EMEP model. The source is defined spatially as the FUA where emissions are reduced yearly ( $Y$  subscript). The receptor is defined as the city location where the maximum yearly averaged concentration is modelled ( $\bar{x}_{max}$ ), and temporally as daily average ( $\bar{D}$ ). Each column represents the number of days with a specific PI difference ( $PI_{100} - PI_{20}$ ). The blue line provides the yearly average difference.

### 386 3.3 Sensitivity to the source

387 Figure 4 shows the comparison between SA obtained with sources defined as core cities (left)  
388 and as FUA (right). The city contribution / responsibility is multiplied by a factor 2 on average  
389 (see also Figure 8) when FUA are considered. The larger spatial extension of the FUA and its  
390 implied additional emissions explain the differences that lead some cities to become a major  
391 actor, i.e. where the city contribution dominates the background one (e.g. Athens, Warsaw,  
392 Milan, Turin and Rome).  
393



394  
395  
396  
397  
398  
399  
Figure 4: Maps of city contributions obtained for spatial sources defined in 2 ways: core city (CC, left) and FUA (right). Results are shown for 150 cities in Europe, based on the SHERPA-CHIMERE model using a potential impact SA method for a reduction strength of 50% ( $PI_{50}$ ). The indicator is the total  $PM_{2.5}$  concentration. The receptor is selected as the location where the maximum yearly average concentration occurs ( $\bar{x}_{max}$ ) and applies yearly time average ( $\bar{Y}$ ). The source emissions are reduced over a full year ( $Y$ ).

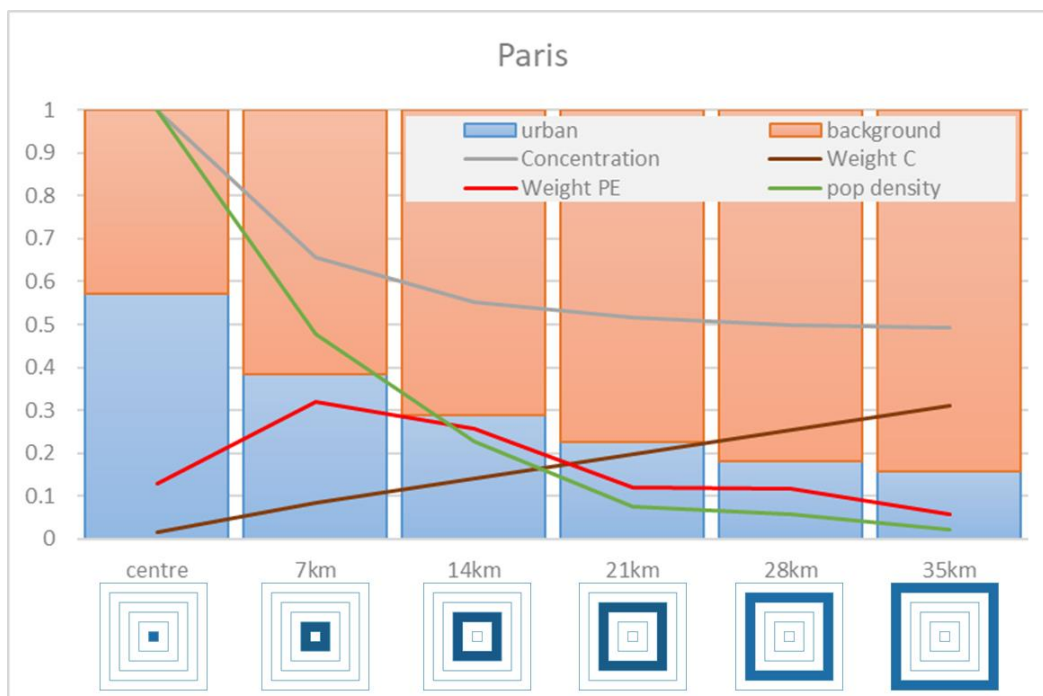
### 400 3.4 Sensitivity to the receptor

401 In this section, we discuss the spatial and temporal averages applied at the receptor. Spatially,  
402 different averaging options exist, ranging from a single location (i.e. one modelling grid cell) to  
403 more or less extended areas covering part of the source or even larger. To illustrate the



404 sensitivity of SA to that choice, we use the case of Paris (Figure 5) where emission have been  
405 reduced over the FUA (source) over a full year.

406  
407 SA varies largely from one location to another within Paris. We highlight this with bars that  
408 distinguish the city vs. background contributions for locations at different distance from the city  
409 centre. We note opposite trends, dominated by the city source (around 60%) at the city center  
410 and dominated by the background source towards the periphery (around 80%). While the SA at  
411 the city centre is representative of a single cell within the city, this is not the case for SA close to  
412 the periphery. This is highlighted by the city rings (below the X-axis) that indicate the area of  
413 representativeness of a given SA. When we average spatially an indicator ( $PM_{2.5}$  or population  
414 exposure) over a receptor that covers the entire FUA (all 6 rings), these areas of  
415 representativeness enter into play. The brown curve indicates the weight (in the spatial average)  
416 attached to each city ring, relatively to the city total (i.e. all rings). Weights increase fast when  
417 moving towards the periphery because of the larger ring areas. The spatial averaging process  
418 leads to over-representing the periphery, which overweight the city center SA by almost a factor  
419 40. It is interesting and counter-intuitive to note that with this averaging process, the city  
420 responsibility decreases when the city area increases. With population exposure as indicator  
421 (weights shown by red curve), the rapid population density decrease balances the ring area  
422 increase when moving outward, leading to weights that dominate for middle rings. It is  
423 interesting to note, that with average population exposure, the city center weight is yet similar to  
424 the weight obtained 28 km away.  
425



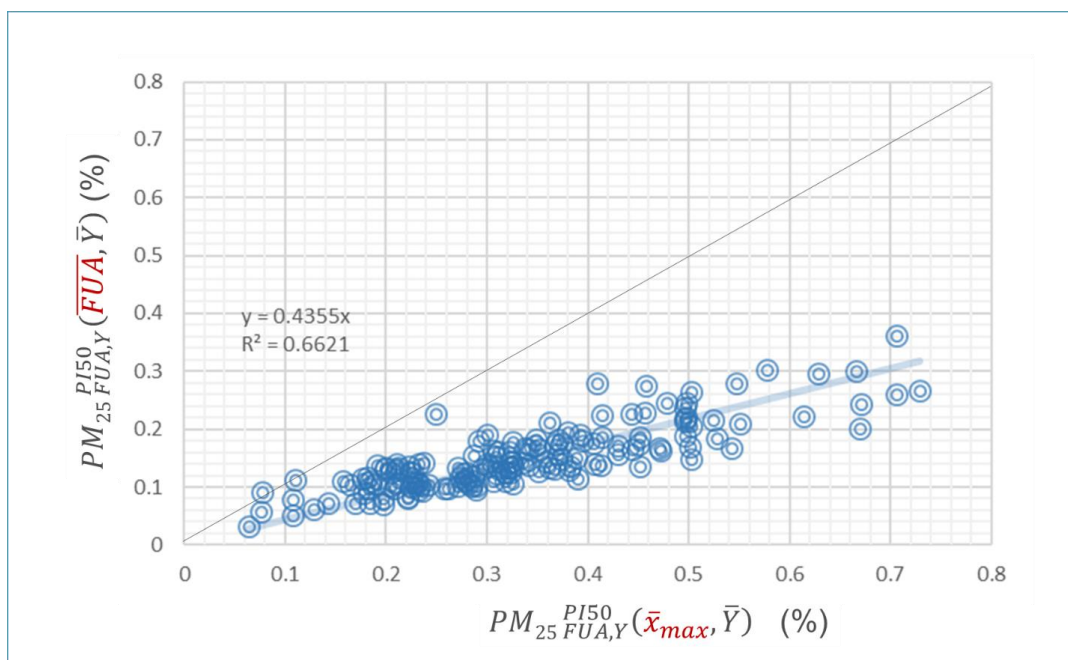
426  
427  
428  
429

Figure 5: City rings' source apportionment for Paris  $PM_{2.5}$  and associated population exposure. The city/background apportionment (bars) is represented for rings (i) progressively more distant from the city centre (X axis). The ring average concentration (C) and population density (P) relative to the city centre values are represented in blue and green, respectively.



430 The relative (to the FUA total, i.e. all rings) weight of each ring ( $i$ ) in the city average concentration (brown) is calculated as  
431  $C_i * S_i / \sum_i (C_i * S_i)$  where  $S_i$  is the ring area, respectively. A similar expression:  $C_i * S_i * P_i / \sum_i (C_i * S_i * P_i)$  is used to determine  
432 the weight of each ring in the calculation of the average population exposure (red curve).

433 Figure 6 compares SA for 150 cities obtained for receptors defined (1) as the location where the  
434 maximum concentration is reached within the FUA ( $\bar{x}_{max}$ ) and (2) as the FUA spatial average  
435 ( $\overline{FUA}$ ). In average, city impacts for a spatially averaged receptor are about 55% lower.  
436 Depending on the spatial characteristic of the receptor, some cities will be considered as minor or  
437 major actors with respect to their pollution. We discuss this issue further in Section 4.  
438

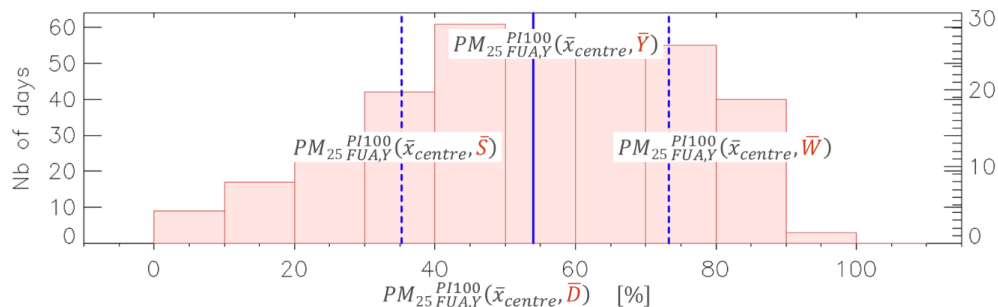


439  
440 Figure 6: Comparison of potential impacts for 150 cities in Europe obtained for a receptor spatially defined as the location where  
441 the concentration is maximum in the city ( $\bar{x}_{max}$  – X axis) and defined as the FUA spatial averaged ( $\overline{FUA}$ ). For these calculations,  
442 the source are defined as the FUA over which emissions are switched off during the whole year. The indicator is the total  $PM_{2.5}$   
443 mass. All results are based on the SHERPA-CHIMERE model using a potential impact SA method for a reduction strength of 50%  
444 (PI50) and are based on yearly averages at the receptor ( $\bar{Y}$ ).

445 As seen from these results, spatial averages at the receptor significantly reduce the city  
446 responsibility, potentially leading to underestimating the city ability to reduce pollution levels  
447 via local controls. The large differences resulting from the choice of the receptor settings prevent  
448 meaningful comparisons. It is for example challenging to compare CAMS city contributions that  
449 are averaged spatially over the city area with the urban results obtained in the context of the  
450 Thematic Strategy on Air Pollution (Kiesewetter and Amann 2014) that are aggregated at  
451 country level or with SHERPA estimates based on a single grid cell receptor. It is therefore  
452 crucial to associate all SA settings (metadata) to the results in order to inform on the  
453 meaningfulness of a comparison. We discuss further this issue in the context of air quality  
454 planning in Section 4.  
455



456 Similar considerations apply to temporal averages. Figure 7 compares SA obtained when the  
457 indicator at the receptor is averaged yearly and seasonally with daily single values. For a yearly  
458 average, Madrid city's contribution is 54% but the spectra of daily contributions show variations  
459 that range from 10 to beyond 90%. Even seasonal averages show important differences with a  
460 factor 2 between summer and winter. Similarly, to spatial averages, temporal averages  
461 encompass a large spectra of SA outcome. Indicators averaged yearly at the receptor have been  
462 used for example in SHERPA (Thunis et al. 2017), GAINS (Kiesewetter and Amann, 2014)  
463 whereas daily indicators are used in CAMS (Pommier et al., 2020).  
464 Note that spatial averages have a larger smoothing effect than temporal ones because they are  
465 bidimensional.  
466



467  
468 *Figure 7: Frequency histogram of daily potential impact at 100% (PI100) modelled with the EMEP model for the city of Madrid.*  
469 *Each column represents the number of days with a given daily PI. The blue line provides the yearly average PI. For these*  
470 *calculations, the source is the Madrid Functional Urban Area (FUA) over which emissions are switched off during the whole year*  
471 *(Y). The indicator is the total PM<sub>2.5</sub> mass. The receptor point is the city centre location ( $\bar{x}_{centre}$ ).*

472

### 473 3.5 Assumptions and uncertainties

474 Most SA methods rely on models and are therefore characterized by a set of common strengths  
475 and weaknesses. One of the main limitations attached to models is the spatial resolution and its  
476 potential impact on the calculation of the city contribution. While a coarse resolution might be  
477 able to capture relatively well the background (characterized by smoother fields), this will not be  
478 the case for peak concentrations within the city. The coarser the model spatial resolution, the  
479 largest the underestimation of the city responsibility will be (De Meij et al., 2007).

480

481 Uncertainties may also result from our incomplete knowledge of some model input parameters,  
482 in particular chemical processes and emission sources. Some urban emission sources are not well  
483 documented and are probably underestimated. This is the case of residential emissions for which  
484 the inclusion of condensable remains a question mark (Bessagnet and Allemand, 2020, Simpson  
485 et al., 2020) or for the resuspension of particles generated by vehicles (Amato et al., 2014).  
486 These lacking or incomplete emission sources will lead to a potential underestimation of the city  
487 responsibility as well.

488

489 In the next section, we discuss the consequences of these results on policy, in particular when SA  
490 information is used to design air quality plans.



#### 491 4. Implications for air quality strategies

492 Estimating the contribution of a city to its pollution has important consequences in terms of air  
493 quality management. Indeed, an important city contribution will be a logic argument to support  
494 substantial control measures at the local level to abate pollution. The effectiveness of the control  
495 measures then relies on the relevance and accuracy of this city contribution; over- or under-  
496 estimated city contributions potentially leading to inefficient measures.

497 In previous sections, we have seen that the city contribution largely varies depending on the  
498 choices made for the SA setting parameters (definition of the indicator, source, receptor and  
499 methodology), hence the challenge to obtain a relevant and accurate estimate to support local  
500 action.

501 Given the range of possible SA options and their impact on results, the first recommendation is  
502 obviously to report these SA setting choices together with the results to provide policymakers  
503 with the full picture and allow them to take informed decisions. This advocates for the use of the  
504 proposed nomenclature or a similar one that documents for the choices in the SA approach,  
505 providing accountability to the method and enabling correct interpretation of the results. The  
506 proposed nomenclature can be understood as a documentation of the SA metadata information.  
507 Apart from this point on the importance of documenting SA approach choices, we show below  
508 that some of the SA settings are fixed by the purpose of the study. We provide suggestions for  
509 the remaining free choices.

510

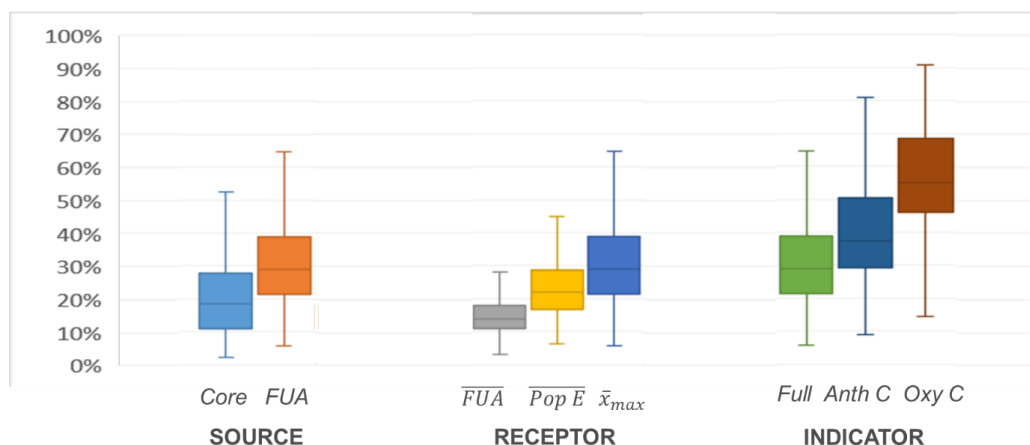
##### 511 The recommended SA method is potential impacts (PI)

512

513 It is important to recall that not all SA methodologies are equally suited to support air quality  
514 planning. As mentioned by several authors (Burr and Zhang 2011, Qiao et al. 2018, Mertens et  
515 al. 2019, Clappier et al. 2017, Grewe et al. 2010, 2012; Thunis et al. 2019), potential impacts are  
516 recommended when non-linear species are involved (which is the case for PM<sub>2.5</sub> and PM<sub>10</sub> but  
517 also for other species like NO<sub>2</sub> or O<sub>3</sub>). It is worth reminding that tagging or incremental  
518 approaches are yet erroneously used and believed to be suited for air quality planning purposes  
519 (Qiao et al. 2018; Guo et al. 2017; Itahashi et al. 2017; Timmermans et al. 2017; Wang et al.  
520 2015, Hendriks et al. 2013). Although challenging practical issues are attached to potential  
521 impacts and may be seen as a burden (e.g. lack of additivity, see Appendix), they only reflect the  
522 complexity of the real processes that must be accounted for. Although uncertainties associated to  
523 the PI approach (e.g. imperfect emission inventory), may lead other SA methods to perform  
524 better in some instances because methodological biases compensate uncertainties, this is  
525 however coincidental. While uncertainties can be tackled and reduced to improve the approach,  
526 this is not the case of methodological biases. These points were extensively discussed in Thunis  
527 et al. (2019).

528

529 For the remaining of this section focusing on policy aspects, only potential impact results are  
530 discussed. Fixing the methodology however still leaves free options in terms of indicator,  
531 receptor and source. This is visualized in Figure 8 that summarizes the variability of the SA  
532 results presented in the previous sections (i.e. Figure 2, Figure 4 and Figure 6) for the 150 cities  
533 to these possible choices. Differences in terms of city responsibility reach a factor 2 in average  
534 for each of these remaining parameters with much larger values for some cities.  
535



536  
537  
538  
539  
540

Figure 8: Box quantile diagrams summarizing the city contributions to  $PM_{2.5}$  levels for the 150 EU cities. All results are based on a similar method (potential impacts at 50%), a similar temporal receptor ( $\bar{Y}$ ) but for different choices of city sources (left), receptors (centre) and indicators (right). See previous sections for details. The two extremities of each vertical line represent the 10<sup>th</sup> and 90<sup>th</sup> percentile contributions among the 150 cities, respectively. The box crossing horizontal line represents the median.

541

#### 542 INDICATOR: The indicator choice is driven by health and environmental objectives

543

544 The choice of the indicator is generally motivated by health or environmental considerations.  
545 Currently, the WHO guidelines (WHO2005) refer to the total  $PM_{2.5}$  mass as the indicator  
546 correlating best with health impacts. These guidelines (or the AAQD limit values) are then the  
547 logical and most relevant indicator choice among the options presented in Section 3.1 and shown  
548 in Figure 2. As illustrated by Figure 8, evolving knowledge on health-related pollution impacts  
549 (i.e. the increased toxicity of some  $PM_{2.5}$  constituents like those related to the traffic and  
550 residential activities) might however, drive the choice towards more detailed indicators (e.g.  
551  $PPM_{2.5}$ ) leading to an increased responsibility for the cities.

552

#### 553 SOURCE: Importance of matching sources with governance levels

554

555 Figure 8 shows that plans limited to city cores would be significantly less efficient than if applied  
556 at the FUA scale. In average over all cities, the efficiency decreases by a factor 2 but larger  
557 differences occur in many cities. The source does however not represent a free choice in the  
558 context of policy practice. Indeed, authorities in charge of AQ plans only have power to act on  
559 the area under their responsibility, which sets where measures apply. The same applies for the  
560 source temporal characteristic, fixed as the period of time during which measures apply. A good  
561 match between the SA settings and the temporal and spatial characteristics of the source is  
562 therefore important to provide meaningful support to policy makers.

563

#### 564 RECEPTOR: Drawbacks associated to spatial and temporal averaging processes at the receptor

565

566 As clearly shown in Figure 5, spatial averaging processes lead to a loss of information. In our  
567 example, a city average based SA would totally occult the city center SA. It would lead to a  
568 strategy that mostly targets the background at the expense of the city center, where the high





569 concentration issues would not be solved. This is well illustrated by Amann et al. (2017) who  
570 analyse the responsibility of the city of New Delhi on its air pollution, both at a city center hot-  
571 spot receptor and in terms of city average population exposure. In the first case, SA suggests  
572 acting on local sources while in the second SA suggests acting on regional sources. Spatial  
573 averaging drives the balance towards regional actions that will less effective in solving the  
574 pollution issue at the city center. The larger the city, the more important this shift will be. As  
575 illustrated by Figure 8, there is more than a factor 2 between city-averaged and hot spot  
576 indicators. Similar considerations apply to temporal averages. Figure 7 clearly shows that yearly  
577 average values hide the potential for effective local actions during wintertime and even more on  
578 specific days.

579  
580 Averaging implies merging, into one single number, locations and time instants that are  
581 characterized by different and sometimes opposite SA. This may lead to strategies that will not  
582 be efficient everywhere all the time. Whenever the final objective is to reduce a temporally  
583 or/and spatially averaged indicator (e.g. average population exposure), strategies would gain in  
584 efficiency with the following process: (1) perform SA and hierarchize the raw (not averaged) SA  
585 results into homogeneous spatio-temporal clusters; (2) design strategies on the basis of these  
586 clusters; (3) assess the strategy efficiency against the averaged indicator. The key is here to  
587 design strategies on raw or clustered results rather than on averaged ones, to prevent information  
588 loss.

589  
590 Note that designing a unique strategy based on multiple SA results (point 2 above) does not  
591 necessarily complicate the analysis, as these different SA will likely suggest action on different  
592 sectors of activity that can be combined at the final strategy.  
593

## 594 5. Conclusions

595 Although air quality has improved in Europe over the last decades, in great part thanks to  
596 effective measures and consistent EU-wide legislation, pollution hot spots yet remain in many  
597 European cities. The extent by which city emissions are causing these elevated urban pollution  
598 levels is however still a subject of scientific discussion. Source apportionment represents a useful  
599 technique to quantify the city responsibility but the approaches and applications are however not  
600 harmonized, therefore not comparable, resulting in confusing and sometimes contradicting  
601 interpretations.

602  
603 In this work, we analyzed how different SA approaches apply to the urban scale and how their  
604 building elements and parameters are defined and set. We identified the possible settings  
605 associated to four key steps in SA: indicator, receptor, source and methodology. We showed that  
606 different choices for these settings lead to very large differences in terms of results. In average  
607 over the 150 European large cities selected as example, the choices made for the indicator, the  
608 receptor, and the source each lead to an average factor 2 difference in terms of city  
609 responsibility. These various options and the large differences that result, highlight the difficulty  
610 of comparing results from different studies and stress the need to document the SA approach  
611 with its related metadata – that documents the choices made for the key four steps.  
612



613 This work advocates for the use of a harmonized nomenclature to support the comparability of  
614 SA approaches. We propose the use of indexes and subindexes attached to the 4 key steps in any  
615 SA approach in a harmonized way to uniquely document the approach and enable correct  
616 interpretation of the results. We believe that the adoption of this nomenclature will provide  
617 clarity to the scientific discussion on different results and enable the correct interpretation of the  
618 results for policy applications. Even though this is applied to the specific case of PM<sub>2.5</sub>, the  
619 concepts presented here can easily be generalized to other pollutants.

620  
621 In the context of supporting urban air quality plans, the SA configuration and most setting  
622 parameters are driven by the purpose of the AQ plan itself and by its associated constraints.  
623 While environmental and/or health related considerations guide the choice of the indicator, the  
624 spatio-temporal characteristics of the source are strongly correlated to governance aspects. In  
625 other words, the source characteristics should reflect the governance levels to facilitate  
626 interpretation. Finally, the recommended SA method should be based on “potential impacts”, to  
627 prevent misleading interpretations in terms of expected AQ plan outcome.

628  
629 At the receptor level, temporal and spatial averaging processes lead to a loss of information,  
630 especially when diverging SA results are aggregated into a single number. Averaging process, in  
631 particular spatial, often lead to favor strategies that target background sources while neglecting  
632 actions that would be efficient at the city center. In our 150 cities example, the impact of spatial  
633 averaging leads to an average factor 2 difference in terms of city responsibility. Not only results  
634 differ from one city to the other, and from one location to another in a given city, they also differ  
635 through time. To cope with this variability, we recommend using non-averaged SA results for the  
636 design of AQ strategies. Once clustered in homogeneous spatio-temporal classes, these can serve  
637 to understand where and when actions are most efficient. When implemented, the efficiency of  
638 abatement measures can then be assessed via spatially and temporally averaged indicator (e.g.  
639 city average population exposure).

640  
641 The responsibility of a city to its pollution is obviously city dependent. But even for a given city,  
642 SA studies using different approaches and parameter settings will deliver very different  
643 outcomes. It is important to note that a departure from the methodological recommendations  
644 listed above, additional uncertainties and assumptions will most often lead to a systematic and  
645 important underestimation of the city responsibility. We showed that in average over 150  
646 European cities, departures in terms of source, receptor, and indicator may lead for each to a  
647 factor 2 underestimation. This comes with important implications: if cities are seen as a minor  
648 actor, plans will target in priority the background at the expense of potentially effective local  
649 actions.

650  
651 Future work will consist in comparing spatially/temporally averaged SA results with SA results  
652 that are clustered in homogeneous spatio-temporal classes and assess the implications in terms of  
653 AQ strategy.

654

## 655 [Acknowledgements](#)

656 The Authors thank Chloé Thunis for her support with the infographics

657

658



## 659 References

- 660 Alberti, V., Alonso Raposo, M., Attardo, C., Auteri, D., Ribeiro Barranco, R., Batista E Silva, F.,  
661 Benczur, P., Bertoldi, P., Bono, F., Bussolari, I., Louro Caldeira, S., Carlsson, J.,  
662 Christidis, P., Christodoulou, A., Ciuffo, B., Corrado, S., Fioretti, C., Galassi, M.,  
663 Galbusera, L., Gawlik, B., Giusti, F., Gomez Prieto, J., Grosso, M., Martinho Guimaraes  
664 Pires Pereira, A., Jacobs, C., Kavalov, B., Kompil, M., Kucas, A., Kona, A., Lavallo, C.,  
665 Leip, A., Lyons, L., Manca, A., Melchiorri, M., Monforti-Ferrario, F., Montalto, V.,  
666 Mortara, B., Natale, F., Panella, F., Pasi, G., Perpia Castillo, C., Pertoldi, M., Pisoni, E.,  
667 Roque Mendes Polvora, A., Rainoldi, A., Rembges, D., Rissola, G., Sala, S., Schade, S.,  
668 Serra, N., Spirito, L., Tsakalidis, A., Schiavina, M., Tintori, G., Vaccari, L., Vandyck, T.,  
669 Vanham, D., Van Heerden, S., Van Noordt, C., Vespe, M., Vettors, N., Vilahur  
670 Chiaraviglio, N., Vizcaino, M., Von Estorff, U. and Zulian, G., The Future of Cities,  
671 Vandecasteele, I., Baranzelli, C., Siragusa, A. and Aurambout, J. editor(s), EUR 29752  
672 EN, Publications Office of the European Union, Luxembourg, 2019, ISBN 978-92-76-  
673 03847-4, doi:10.2760/375209, JRC116711.
- 674 Amann, M., Pallav Purohit, Anil D. Bhanarkar, Imrich Bertok, Jens Borcken-Kleefeld, Janusz  
675 Cofala, Chris Heyes, Gregor Kiesewetter, Zbigniew Klimont, Jun Liu, Dipanjali  
676 Majumdar, Binh Nguyen, Peter Rafaj, Padma S. Rao, Robert Sander, Wolfgang Schöpp,  
677 Anjali Srivastava, B. Harsh Vardhan, 2017. Managing future air quality in megacities: A  
678 case study for Delhi, Atmospheric Environment, 161, 99-111.
- 679 AQD, 2008. Directive 2008/50/EC of the European Parliament and of the Council of 21 May  
680 2008 on ambient air quality and cleaner air for Europe (No. 152). Official Journal.
- 681 Amato, F., Cassee, F.R., Denier van der Gon, H.A.C., Gehrig, R., Gustafsson, M., Hafner, W.,  
682 Harrison, R.M., Jozwicka, M., Kelly, F.J., Moreno, T., Prevot, A.S.H., Schaap, M.,  
683 Sunyer, J., Querol, X., 2014. Urban air quality: The challenge of traffic non-exhaust  
684 emissions. Journal of Hazardous Materials 275, 31–36.  
685 <https://doi.org/10.1016/j.jhazmat.2014.04.053>
- 686 ATMO2003: L'indice ATMO: indicateur de la qualité de l'air dans les agglomérations françaises  
687 [The ATMO index: an air quality indicator for developed areas in France]. Eur Ann  
688 Allergy Clin Immunol. 2003 May;35(5):166-9. French. PMID: 12838780.
- 689 ApSimon H., T. Oxley, H. Woodward, D. Mehlig, A. Dore, M. Holland, 2021. The UK  
690 Integrated Assessment Model for source apportionment and air pollution policy  
691 applications to PM2.5, Environment International, 153, 106515.
- 692 Belis, C.A., D. Pernigotti, G. Pirovano, O. Favez, J.L. Jaffrezo, J. Kuenen, H. Denier van Der  
693 Gon, M. Reizer, V. Riffault, L.Y. Alleman, M. Almeida, F. Amato, A. Angyal, G.  
694 Argyropoulos, S. Bande, I. Beslic, J.-L. Besombes, M.C. Bove, P. Brotto, G. Calori, D.  
695 Cesari, C. Colombi, D. Contini, G. De Gennaro, A. Di Gilio, E. Diapouli, I. El Haddad,  
696 H. Elbern, K. Eleftheriadis, J. Ferreira, M. Garcia Vivanco, S. Gilardoni, B. Golly, S.  
697 Hellebust, P.K. Hopke, Y. Izadmanesh, H. Jorquera, K. Krajsek, R. Kranenburg, P.  
698 Lazzeri, F. Lenartz, F. Lucarelli, K. Maciejewska, A. Manders, M. Manousakas, M.  
699 Masiol, M. Mircea, D. Mooibroek, S. Nava, D. Oliveira, M. Paglione, M. Pandolfi, M.  
700 Perrone, E. Petralia, A. Pietrodangelo, S. Pillon, P. Pokorna, P. Prati, D. Salameh, C.  
701 Samara, L. Samek, D. Saraga, S. Sauvage, M. Schaap, F. Scotto, K. Sega, G. Siour, R.  
702 Tauler, G. Valli, R. Vecchi, E. Venturini, M. Vestenius, A. Waked, E. Yubero, 2020.  
703 Evaluation of receptor and chemical transport models for PM10 source apportionment,  
704 Atmospheric Environment: X, 5,100053.



- 705 Bhave P.V., Pouliot G.A. and Zheng M., 2007. Diagnostic model evaluation for carbonaceous  
706 PM<sub>2.5</sub> using organic markers measured in the southeastern U.S. *Environmental Science*  
707 *and Technology* 41, 1577-1583.
- 708 Burr M.J. and Y. Zhang, 2011b. Source apportionment of fine particulate matter over the Eastern  
709 U.S. Part II: source sensitivity simulations using CAMX/PSAT and comparisons with  
710 CMAQ source sensitivity simulations, *Atmospheric Pollution Research*, 2, 318-336
- 711 Clappier A., E. Pisoni, P. Thunis, 2015. A new approach to design source–receptor relationships  
712 for air quality modelling. *Environmental Modelling & Software*, 74, 66-74.
- 713 Clappier A., C. Belis, D. Pernigotti and P. Thunis (2017) Source apportionment and sensitivity  
714 analysis: two methodologies with two different purposes. *Geosci. Model Dev. Discuss.*,  
715 <https://doi.org/10.5194/gmd-2017-161>, in review, 2017.
- 716 de Bruyn, S., de Vries, J., 2020. Health costs of air pollution in European cities and the linkage  
717 with transport (No. 20.190272.134). CE Delft, Delft.
- 718 Degraeuwe, B., Pisoni, E., Peduzzi, E., De Meij, A., Monforti-Ferrario, F., Bodis, K.,  
719 Mascherpa, A., Astorga-Llorens, M., Thunis, P. and Vignati, E., *Urban NO<sub>2</sub> Atlas*, EUR  
720 29943 EN, Publications Office of the European Union, Luxembourg, 2019, ISBN 978-  
721 92-76-10386-8 (online), 978-92-76-10387-5 (print), doi:10.2760/43523  
722 (online), 10.2760/538816 (print), JRC118193.
- 723 De Meij, A., S. Wagner, N. Gobron, P. Thunis, C. Cuvelier, F. Dentener, M. Schaap, Model  
724 evaluation and scale issues in chemical and optical aerosol properties over the greater  
725 Milan area (Italy), for June 2001, *Atmos. Res.* 85, 243-267, 2007.
- 726 European Environment Agency. *Air Quality in Europe: 2020 Report*. Publications Office, 2020.  
727 DOI.org (CSL JSON), <https://data.europa.eu/doi/10.2800/786656>.
- 728 European Environment Agency, *Air quality in Europe — 2017 report*, No13/2017, ISSN 1977-  
729 8449, doi:10.2800/850018, [https://www.eea.europa.eu/publications/air-quality-in-europe-](https://www.eea.europa.eu/publications/air-quality-in-europe-2017)  
730 2017.
- 731 European Commission. Joint Research Centre. Institute for Energy and Transport., 2014. Non-  
732 exhaust traffic related emissions - Brake and tyre wear PM: literature review.  
733 Publications Office, LU.
- 734 Grewe, V., E. Tsati, P. Hoor, 2010. On the attribution of contributions of atmospheric trace gases  
735 to emissions in atmospheric model applications, *Geosci. Model Dev.*, 3, 487-499
- 736 Grewe, V., K. Dahlmann, S. Matthes, W. Steinbrecht, 2012. Attributing ozone to NO<sub>x</sub>  
737 emissions: Implications for climate mitigation measures, *Atmos. Environ.*, 59, 102-107
- 738 Guo H., S. H. Kota, S. K. Sahu, J. Hu, Q. Ying, A. Gao, H. Zhang, 2017. Source apportionment  
739 of PM<sub>2.5</sub> in North India using source-oriented air quality models. *Environmental*  
740 *Pollution* 231, 426-436.
- 741 Hendriks C., R. Kranenburg, J. Kuenen, R. van Gijlswijk, R. Wichink Kruit, A. Segers, H.  
742 Denier van der Gon, M. Schaap, 2013. The origin of ambient particulate matter  
743 concentrations in the Netherlands, *Geosci. Model Dev.*, 6, 721–733, 2013
- 744 Huang Y., T. Deng, Z. Li, N. Wang, C. Yin, S. Wang, S. Fan, 2018. Numerical simulations for  
745 the sources apportionment and control strategies of PM<sub>2.5</sub> over Pearl River Delta, China,  
746 part I: Inventory and PM<sub>2.5</sub> sources apportionment, *Science of the Total Environment*  
747 634 (2018) 1631–1644.
- 748 Itahashi S., H. Hayami, K. Yumimoto, I. Uno, 2017. Chinese province-scale source  
749 apportionments for sulfate aerosol in 2005 evaluated by the tagged tracer method,  
750 *Environmental Pollution* 220, 1366-1375.



- 751 Kaspar R. Daellenbach, Gaëlle Uzu, Jianhui Jiang, Laure-Estelle Cassagnes, Zaira Leni,  
752 Athanasia Vlachou, Giulia Stefanelli, Francesco Canonaco, Samuël Weber, Arjo Segers,  
753 Jeroen J. P. Kuenen, Martijn Schaap, Olivier Favez, Alexandre Albinet, Sebnem  
754 Aksoyoglu, Josef Dommen, Urs Baltensperger, Marianne Geiser, Imad El Haddad, Jean-  
755 Luc Jaffrezo, André S. H. Prévôt. Sources of particulate-matter air pollution and its  
756 oxidative potential in Europe. *Nature*, 2020; 587 (7834): 414 DOI: 10.1038/s41586-020-  
757 2902-8
- 758 Keuken M., M. Moerman, M. Voogt, M. Blom, E.P. Weijers, T. Röckmann, U. Dusek (2013)  
759 Source contributions to PM<sub>2.5</sub> and PM<sub>10</sub> at an urban background and a street location,  
760 *Atmos. Environ.*, 71, 26–35.
- 761 Khomenko, S., Cirach, M., Pereira-Barboza, E., Mueller, N., Barrera-Gómez, J., Rojas-Rueda,  
762 D., de Hoogh, K., Hoek, G., Nieuwenhuijsen, M., 2021. Premature mortality due to air  
763 pollution in European cities: a health impact assessment. *The Lancet Planetary Health*  
764 S2542519620302722. [https://doi.org/10.1016/S2542-5196\(20\)30272-2](https://doi.org/10.1016/S2542-5196(20)30272-2)
- 765 Kieseewetter G. and Amann (2014). Urban PM<sub>2.5</sub> levels under the EU Clean Air Policy Package,  
766 IIASA TSAP Report 12.
- 767 Kieseewetter G., J. Borken-Kleefeld, W. Schöpp, C. Heyes, P. Thunis, B. Bessagnet, E.  
768 Terrenoire, H. Fagerli, A. Nyiri and M. Amann (2015) Modelling street level PM<sub>10</sub>  
769 concentrations across Europe: source apportionment and possible futures, *Atmos. Chem.*  
770 *Phys.*, 15, 1539-1553.
- 771 Kranenburg R., Segers A., Hendriks C., and Schaap., 2013. Source apportionment using  
772 LOTOS-EUROS: module description and evaluation, *Geosci. Model Dev.*, 6, 721–733
- 773 Kole, P.J., Löhr, A.J., Van Belleghem, F., Ragas, A., 2017. Wear and Tear of Tyres: A Stealthy  
774 Source of Microplastics in the Environment. *IJERPH* 14, 1265.  
775 <https://doi.org/10.3390/ijerph14101265>
- 776 Kwok R.H.F., S.L. Napelenok, K.R. Baker, 2013: Implementation and evaluation of PM<sub>2.5</sub>  
777 source contribution analysis in a photochemical model, *Atmospheric Environment* 80,  
778 398-407
- 779 Lavallo, C., Pontarollo, N., Batista E Silva, F., Baranzelli, C., Jacobs, C., Kavalov, B., Kompil,  
780 M., Perpiña Castillo, C., Vizcaino, M., Ribeiro Barranco, R., Vandecasteele, I., Pinto  
781 Nunes Nogueira Diogo, V., Aurambout, J., Serpieri, C., Marín Herrera, M., Rosina, K.,  
782 Ronchi, S. and Auteri, D., *European Territorial Trends - Facts and Prospects for Cities*  
783 *and Regions* Ed. 2017, EUR 28771 EN, Publications Office of the European Union,  
784 Luxembourg, 2017, ISBN 978-92-79-79906-8, doi:10.2760/28183, JRC107391.
- 785 Lenschow P., H.-J. Abraham, K. Kutzner, M. Lutz, J.-D. Preu, W. Reichenbacher (2001) Some  
786 ideas about the sources of PM<sub>10</sub>, *Atmospheric Environment* 35 Supplement No. 1 23–33.
- 787 Li Y., D. K. Henze, D. Jack, B. H. Henderson, P. L. Kinney, 2016. Assessing public health  
788 burden associated with exposure to ambient black carbon in the United States, *Science of*  
789 *the Total Environment* 539, 515–525.
- 790 Fei Liu, Z. Klimont, Qiang Zhang, J. Cofala, Lijian Zhao, Hong Huo, B. Nguyen, W. Schöpp, R.  
791 Sander, Bo Zheng, Chaopeng Hong, Kebin He, M. Amann, Ch. Heyes, 2013. Integrating  
792 mitigation of air pollutants and greenhouse gases in Chinese cities: development of  
793 GAINS-City model for Beijing, *Journal of Cleaner Production*, Volume 58, 25-33,  
794 <https://doi.org/10.1016/j.jclepro.2013.03.024>.



- 795 Luo H., L. Yang, Z. Yuan, K. Zhao, S. Zhang, Y. Duan, R. Huang, Q. Fu, 2020. Synoptic  
796 condition-driven summertime ozone formation regime in Shanghai and the implication  
797 for dynamic ozone control strategies, *Science of The Total Environment*, 745, 141130.
- 798 Mertens, M., Volker G., V.S. Rieger and P. Jöckel. Revisiting the contribution of land transport  
799 and shipping emissions to tropospheric ozone, *Atmos. Chem. Phys.*, 18, 5567–5588, 2018
- 800 Ntziachristos, L., Boulter, P., 2019. EMEP/EEA air pollutant emission inventory guidebook  
801 2019 - 1.A.3.b.vi Road transport: Automobile tyre and brake wear - 1.A.3.b.vii Road  
802 transport: Automobile road abrasion. European Environment Agency.
- 803 OECD (2012) Redefining Urban: a new way to measure metropolitan areas, OECD report,  
804 ISBN: 9789264174054, 148pp.
- 805 O'Neill, B. C., Dalton, M., Fuchs, R., Jiang, L., Pachauri, S., Zigova, K., Global demographic  
806 trends and future carbon emissions, *Proceedings of the National Academy of Sciences*  
807 Oct 2010, 107 (41) 17521-17526; DOI: 10.1073/pnas.1004581107.
- 808 Ortiz S. and Friedrich, R.: A modelling approach for estimating background pollutant  
809 concentrations in urban areas, *Atmos. Pollut. Res.*, 4, 147–156,  
810 doi:10.5094/APR.2013.015, 2013.
- 811 Osada, K., Ohara, T., Uno, I., Kido, M., Iida, H., 2009. Impact of Chinese anthropogenic  
812 emissions on submicrometer aerosol concentration at Mt. Tateyama, Japan. *Atmos.*  
813 *Chem. Phys.* 9 (23), 9111–9120.
- 814 Park, M., Joo, H.S., Lee, K. et al. Differential toxicities of fine particulate matters from various  
815 sources. *Sci Rep* 8, 17007 (2018). <https://doi.org/10.1038/s41598-018-35398-0>
- 816 Petetin H. M. Beekmann, J. Sciare, M. Bressi, A. Rosso, O. Sanchez and V. Ghers. (2014) A  
817 novel model evaluation approach focusing on local and advected contributions to urban  
818 PM<sub>2.5</sub> levels – application to Paris, France, *Geosci. Model Dev.*, 7, 1483–1505.
- 819 Pey J., X. Querol and A. Alastuey, 2010, Discriminating the regional and urban contributions in  
820 the North-Western Mediterranean: PM levels and composition, *Atmospheric*  
821 *Environment* 44, 1587-1596.
- 822 Pisoni E., A. Clappier, B. Degrauwe, P. Thunis, 2017. Adding spatial flexibility to source-  
823 receptor relationships for air quality modelling, *Environmental Modelling & Software*,  
824 90, 68-77.
- 825 Pommier, M., Fagerli, H., Schulz, M., Valdebenito, A., Kranenburg, R., and Schaap, M.:  
826 Prediction of source contributions to urban background PM<sub>10</sub> concentrations in European  
827 cities: a case study for an episode in December 2016 using EMEP/MSC-W rv4.15 and  
828 LOTOS-EUROS v2.0 – Part 1: The country contributions, *Geosci. Model Dev.*, 13,  
829 1787–1807, <https://doi.org/10.5194/gmd-13-1787-2020>, 2020.
- 830 Qiao X., Q. Ying, X. Li, H. Zhang, J. Hu, Y. Tang, X. Chen, 2018. Source apportionment of  
831 PM<sub>2.5</sub> for 25 Chinese provincial capitals and municipalities using a source-oriented  
832 Community Multiscale Air Quality model, *Science of the Total Environment* 612, 462–  
833 471.
- 834 Raifman, M., Russell, A. G., Skipper, T. N., & Kinney, P. L. (2020). Quantifying the health  
835 impacts of eliminating air pollution emissions in the city of Boston. *Environmental*  
836 *Research Letters*, 15(9) doi:10.1088/1748-9326/ab842b
- 837 Schaap, M., Timmermans, R.M.A., Roemer, M., Boersen, G.A.C., Builtjes, P.J.H. Sauter, F.J.,  
838 Velders, G.J.M. and Beck, J.P. (2008) ‘The LOTOS–EUROS model: description,  
839 validation and latest developments’, *Int. J. Environment and Pollution*, Vol. 32, No. 2,  
840 pp.270–290.



- 841 Simpson, D., Benedictow, A., Berge, H., Bergström, R., Emberson, L. D., Fagerli, H., Flechard,  
842 C. R., Hayman, G. D., Gauss, M., Jonson, J. E., Jenkin, M. E., Nyíri, A., Richter, C.,  
843 Semeena, V. S., Tsyro, S., Tuovinen, J.-P., Valdebenito, Á., and Wind, P.: The EMEP  
844 MSC-W chemical transport model – technical description, *Atmos. Chem. Phys.*, 12,  
845 7825–7865, <https://doi.org/10.5194/acp-12-7825-2012>, 2012.
- 846 Squizzato S. and M. Masiol (2015) Application of meteorology-based methods to determine  
847 local and external contributions to particulate matter pollution: A case study in Venice  
848 (Italy), *Atmospheric Environment* 119, 69-81.
- 849 Timmermans R.M.A., H.A.C. Denier van der Gon, J.J.P. Kuenen, A.J. Segers, C. Honoré, O.  
850 Perrussel, P.J.H. Builtjes and M. Schaap (2013) Quantification of the urban air pollution  
851 increment and its dependency on the use of down-scaled and bottom-up city emission  
852 inventories, *Urban Climate* 6, 44–62.
- 853 UN, 2020 Policy Brief, Covid-19 in an urban world.  
854 [https://www.un.org/sites/un2.un.org/files/sg\\_policy\\_brief\\_covid\\_urban\\_world\\_july\\_2020](https://www.un.org/sites/un2.un.org/files/sg_policy_brief_covid_urban_world_july_2020.pdf)  
855 .pdf
- 856 Thunis, P., Degraeuwe, B., Peduzzi, E., Pisoni, E., Trombetti, M., Vignati, E., Wilson, J., Belis,  
857 C. and Pernigotti, D., *Urban PM2.5 Atlas: Air Quality in European cities*, EUR 28804  
858 EN, Publications Office of the European Union, Luxembourg, 2017, ISBN 978-92-79-  
859 73876-0 (online),978-92-79-73875-3 (print),978-92-79-75274-2 (ePub),  
860 doi:10.2760/336669 (online),10.2760/851626 (print),10.2760/865663 (ePub),  
861 JRC108595.
- 862 Thunis P. (2018). On the validity of the incremental approach to estimate the impact of cities on  
863 air quality, *Atmospheric Environment*, 173, 210-222.
- 864 Thunis P., B. Degraeuwe, E. Pisoni, M. Trombetti, E. Peduzzi, C.A. Belis, J. Wilson, A.  
865 Clappier, E. Vignati, 2018. PM2.5 source allocation in European cities: A SHERPA  
866 modelling study, *Atmospheric Environment*, 187, 93-106.
- 867 Tobías, A., Carnerero, C., Reche, C., Massagué, J., Via, M., Minguillón, M. C., . . . Querol, X.  
868 202). Changes in air quality during the lockdown in barcelona (spain) one month into the  
869 SARS-CoV-2 epidemic. *Science of the Total Environment*, 726  
870 doi:10.1016/j.scitotenv.2020.138540
- 871 Transboundary particulate matter, photo-oxidants, acidification and eutrophication components.  
872 Joint MSC-W & CCC & CEIP Report. EMEP Status Report 1/2017
- 873 United Nations, Department of Economic and Social Affairs, Population Division (2018), *The*  
874 *World's Cities in 2018 – Data Booklet (ST/ESA/SER.A/417)*.
- 875 Van Dingenen R., F. Dentener, M. Crippa, J. Leitao, E. Marmer, S. Rao, E. Solazzo and L.  
876 Valentini, 2018. TM5-FASST: a global atmospheric source-receptor model for rapid  
877 impact analysis of emission changes on air quality and short-lived climate pollutants.  
878 *Atmospheric Chemistry and Physics*, <https://doi.org/10.5194/acp-2018-112>
- 879 Viana, M., Querol, X., Alastuey, A., Ballester, F., Llop, S., Esplugues, A., . . . Herce, M. D.  
880 (2008). Characterising exposure to PM aerosols for an epidemiological study.  
881 *Atmospheric Environment*, 42(7), 1552-1568. doi:10.1016/j.atmosenv.2007.10.087
- 882 Wagstrom, K. M., Pandis, S. N., Yarwood, G., Wilson, G. M., and Morris, R. E., 2008:  
883 Development and application of a computationally efficient particulate matter  
884 apportionment algorithm in a three dimensional chemical transport model, *Atmos.*  
885 *Environ.*, 42, 5650–5659.



- 886 Wang Z. S., Chien C.-J., and Tonnesen G. S., 2009. Development of a tagged species source  
887 apportionment algorithm to characterize three-dimensional transport and transformation  
888 of precursors and secondary pollutants, *J. Geophys. Res.*, 114, D21206
- 889 Wang L., Z. Wei, W. Wei, J. S. Fu, C. Meng, S. Ma, 2015. Source apportionment of PM<sub>2.5</sub> in  
890 top polluted cities in Hebei, China using the CMAQ model, *Atmospheric Environment*  
891 122, 723-736
- 892 Wang, L.T., Wei, Z., Yang, J., Zhang, Y., Zhang, F.F., Su, J., Meng, C.C., Zhang, Q., 2014. The  
893 2013 severe haze over southern Hebei, China: model evaluation, source apportionment,  
894 and policy implications. *Atmos. Chem. Phys.* 14, 3151-3173.
- 895 WHO2005, Air Quality Guidelines Global Update 2005. Particulate matter, ozone, nitrogen  
896 dioxide and sulfur dioxide, ISBN 92 890 2192 6
- 897 Wu, Q.Z., Wang, Z.F., Gbaguidi, A., Gao, C., Li, L.N., Wang, W., 2011. A numerical study of  
898 contributions to air pollution in Beijing during CAREBeijing-2006. *Atmos. Chem. Phys.*  
899 11 (12), 5997–6011.
- 900 Yarwood G., Morris R.E., and Wilson G.M, 2004. Particulate Matter Source Apportionment  
901 Technology (PSAT) in the CAMx Photochemical Grid Model. Proceedings of the 27th  
902 NATO/ CCMS International Technical Meeting on Air Pollution Modeling and  
903 Application. Springer Verlag  
904



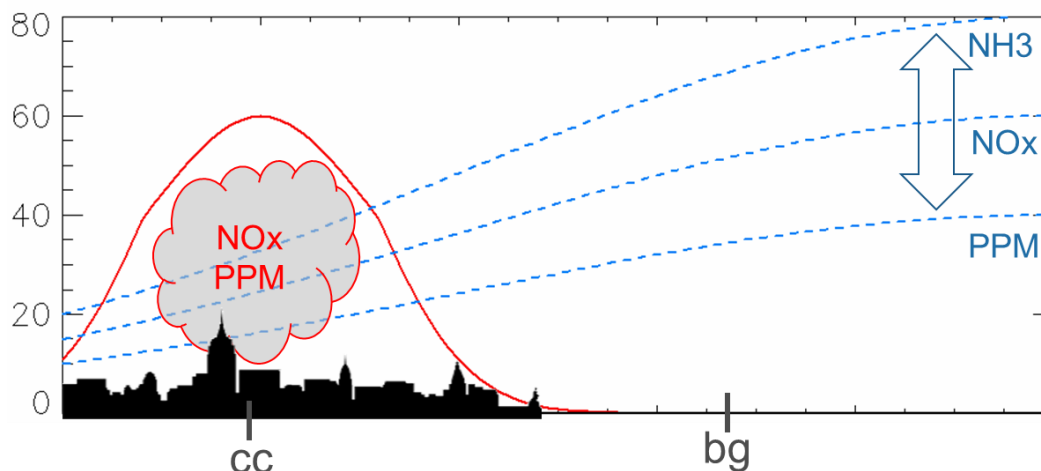


## 905 Appendix A

906 To illustrate the differences among SA methods, we use here the theoretical example  
907 schematically represented in Figure . A city source (in red) emits with a Gaussian dispersion  
908 profile both primary PM (PPM) and a gas-phase precursor ( $\text{NO}_x$ ). The background pollution (in  
909 blue) is composed of a mix of  $\text{NO}_x$ ,  $\text{NH}_3$  and PPM compounds. The various chemical reactions  
910 that take place are simplified here for convenience into a single reaction. One mole of  $\text{NH}_3$  reacts  
911 with one mole of  $\text{NO}_x$  to create one mole of ammonium nitrate ( $\text{NH}_4^+\text{NO}_3^-$ ), i.e. secondary PM.  
912 ( $\text{NO}_x + \text{NH}_3 + X \rightarrow \text{NH}_4^+\text{NO}_3^-$ ). We assume here that the external compounds involved in the  
913 reaction (X) are abundant and do not have a limiting effect on the formation of PM. While the  
914 city emissions (source) remain unchanged, we modify the relative importance of the three  
915 background compounds so that the background becomes in turn PPM,  $\text{NO}_x$  and  $\text{NH}_3$  dominated.  
916 The PM concentration at a given location “x” is given by:

$$917 \quad \text{PM}(x) = \text{PPM}(x) + \min\{\text{NO}_x(x), \text{NH}_3(x)\}_{\text{mole}} \times \text{NH}_4^+\text{NO}_3^- \quad (4)$$

918



919  
920 *Figure A1: Schematic representation of the theoretical example used to compare the three SA approaches. The city source (in*  
921 *red) emits  $\text{NO}_x$  and PPM. The background (in blue, including other cities as well as rural sources) is composed of  $\text{NO}_x$ , PPM and*  
922  *$\text{NH}_3$  in different relative proportions (indicated by the arrow). The “cc” and “bg” symbols represent the city centre receptor and*  
923 *the background location used for the increment approach, respectively.*

924 Based on the formulations provided in Table 1 and equation (4), the expressions to calculate the  
925 city and background components for the theoretical example presented above are detailed in  
926 Table . While these formulations are relatively straightforward for potential impacts and  
927 increments, it is more complex for the tagging method. The city tagging component is the sum of  
928 all PM species that are directly related to the city emissions. This includes PPM and  $\text{NO}_3$  that are  
929 related to the PPM and  $\text{NO}_x$  city emissions, respectively. For the background component, it  
930 includes PPM,  $\text{NO}_x$  and also  $\text{NH}_4$  that is related to the  $\text{NH}_3$  emissions. Tagging allows following  
931 the  $\text{NO}_x$  and  $\text{NH}_3$  emitted compounds through their chemical processes and transformations until  
932 they create  $\text{NO}_3$  and  $\text{NH}_4$ , respectively that can be attributed to their respective sources. As  $\text{NO}_x$   
933 is emitted by both sources, the total  $\text{NO}_3$  must be fractioned and attributed to each single source.



934 In our example, the  $\text{NO}_3$  fraction attributed to the city depends on the ratio of the available  $\text{NO}_x$   
 935 precursor at the location of interest ( $\beta = \frac{\text{NO}_{x\text{city}}(cc)}{\text{NO}_x(cc)}$ ). A similar process is used to calculate the  
 936 background component.

937  
 938 This example is used to compared the increment (INC), tagging (TAG) and potential impact (PI)  
 939 SA approaches.

940  
 941

Potential Impact	
City	$PM_{\text{city}}^{\text{PI}\alpha}(cc) = \frac{PM(cc) - PM_{\text{city}\alpha}(cc)}{\alpha}$
Background	$PM_{\text{bg}}^{\text{PI}\alpha}(cc) = \frac{PM(cc) - PM_{\text{bg}\alpha}(cc)}{\alpha}$
Increment	
City	$PM_{\text{city}}^{\text{INC}}(cc) = PM(cc) - PM(\text{bg})$
Background	$PM_{\text{bg}}^{\text{INC}}(cc) = PM(\text{bg})$
Tagging	
City	$PM_{\text{city}}^{\text{TAG}}(cc) = \sum_E^{\text{city}} PM_E(cc) = PPM_{E(\text{PPM})\text{city}}(cc) + \beta \text{NO}_3^-_{E(\text{NO}_2)\text{city}}(cc)$
Background	$PM_{\text{bg}}^{\text{TAG}}(cc) = \sum_E^{\text{bg}} PM_E(cc) = PPM_{E(\text{PPM})\text{bg}}(cc) + (1 - \beta) \text{NO}_3^-_{E(\text{NO}_2)\text{bg}}(cc) + \text{NH}_4^+_{E(\text{NH}_3)\text{bg}}(cc)$

942 Table A1: Formulations for the potential impacts, increments and tagging approach for the example presented in Figure . The  
 943 indicator for all methods and components is the total particulate matter mass (PM). The SA method is indicated as superscript  
 944 (PI $\alpha$ , INC or TAG) whereas the source (city or bg) is in subscript. The receptor is the city center (cc) while the rural location  
 945 selected for the increment approach is denoted by "bg". For the tagging, the source subscript is also expressed directly as  
 946 emissions (E) distinguishing each compound (within brackets).

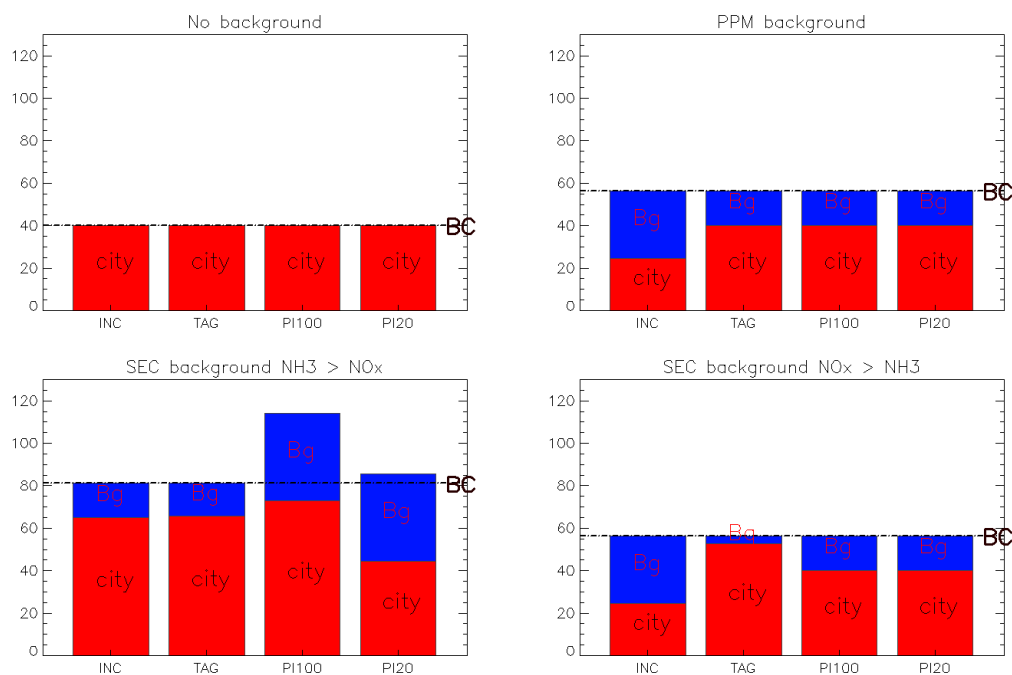
947 Figure shows the city and background contributions obtained with the three SA methods,  
 948 differentiating two options for the PI one: 100% (PI100) and 20% reduction of the sources  
 949 (PI20). The figure also distinguishes four situations characterized by different background  
 950 compositions.

951  
 952  
 953  
 954  
 955  
 956  
 957  
 958  
 959  
 960

1. **No background:** When no background is present (top left), the city  $\text{NO}_x$  emissions do not form PM, only PPM emissions do. In such cases, all methods deliver the same response.
2. **PPM background:** When the background is composed of PPM only (top right), no secondary species are formed. All methods agree with the exception of the increment approach. This is due to the non-fulfilment of one of its underlying assumptions, i.e. the lack of spatial homogeneity of the background which affects differently the rural and city locations (indicated by "cc" and "bg" in Figure , respectively).



- 961 3. SEC background with  $\text{NH}_3 > \text{NO}_x$ : When secondary background precursors ( $\text{NO}_x$  and  
962  $\text{NH}_3$ ) reach the city (bottom row), SA methods deliver different results because they  
963 manage differently non-linear processes. When  $\text{NH}_3$  is more abundant than  $\text{NO}_x$  (bottom  
964 left), the PI100 method does not preserve additivity (discussed in the “concepts” section),  
965 i.e. the sum of the two components exceeds the total PM concentration. As seen from the  
966 results and also from Table , this is not the case for the increment and tagging approaches  
967 that are constructed to be additive.
- 968
- 969 4. SEC background with  $\text{NH}_3 < \text{NO}_x$ : When  $\text{NH}_3$  is less abundant than  $\text{NO}_x$  (bottom right),  
970 differences remain important between the tagging, potential impacts and increment  
971 approaches but additivity is preserved for both PI100 and PI10 that provide identical  
972 responses.



973  
974 *Figure A2: Comparison of the city (red) and background (blue) components for 4 approaches applied on the theoretical examples*  
975 *described in Figure . Results are expressed for different types of background: (top left) no background; (top right) background*  
976 *limited to PPM; (bottom left) background limited to secondary but with  $\text{NH}_3 > \text{NO}_x$ , and (bottom right) background limited to*  
977 *secondary but with  $\text{NH}_3 < \text{NO}_x$ .*